American Mineralogist, Volume 74, pages 1168–1176, 1989

Crystal chemistry and crystallography of some minerals within the pyrite group

Peter Bayliss
Department of Geology and Geophysics, The University of Calgary, Alberta, T2N 1N4, Canada

Abstract

Isotropic pyrite belongs to space group $Pa3$. Anisotropic pyrite, like cobaltite, is interpreted as a sextuplet of interpenetrating, twin-related, orthorhombic (space group $Pca2_1$) domains about a $\bar{3}$ twin axis [111]. The Fe atom in pyrite is considered to move away from the three S atoms with single bonds to Fe and toward the three S atoms with double bonds to Fe. A simple electronic theory for pyrite-type structures is proposed, in which mineral species within the cobaltite subgroup ($Pca2_1$) are semiconductors with a d^6 electronic configuration around the metal nucleus, whereas mineral species within the ullmannite subgroup ($P2_13$) are metallic with a d^7 electronic configuration around the metal nucleus.

A comparison of calculated and observed X-ray powder-diffraction intensities of tolovkite (IrSbS) indicates that tolovkite belongs to the cobaltite subgroup rather than the ullmannite subgroup. The observed X-ray powder-diffraction intensities of maslovite (PtBiTe) agree with the calculated intensities of the pyrite-subgroup model. Penroseite ($NiSe_2$), vaesite (NiS_2), and villamaninite (CuS_2) belong to the pyrite subgroup. Bravoite is a varietal name for nickeloan pyrite, and fukuchilite may be a ferroan villamaninite.

Introduction

Synthesis of the existing data on the crystallography and crystal chemistry of minerals within the pyrite, cobaltite, and ullmannite subgroups suggests certain problems as follows: (1) To find the chemical reasons why some mineral species adopt the ordering scheme of the cobaltite subgroup ($Pca2_1$), whereas other mineral species adopt the ordering scheme of the ullmannite subgroup ($Pa3$). (2) To find the chemical reasons that cause the crystal structure of anisotropic pyrite to deviate from cubic symmetry. (3) To determine the subgroups of minerals such as tolovkite (IrSbS) and maslovite (PtBiTe). (4) To determine the space group of minerals such as penroseite ($NiSe_2$), vaesite (NiS_2), and villamaninite (CuS_2). (5) To define the range in chemical composition of villamaninite (CuS_2). (6) To ascertain the status of minerals within the pyrite subgroup such as bravoite, $(Fe,Ni)S_2$, and fukuchilite, $(Cu,Fe)S_2$.

Subgroups

Octahedral sites are often distorted from O_h symmetry by two limiting types of distortion (Robinson et al., 1971). Trigonal distortion of the octahedron along an S_6 axis by compression or elongation creates a trigonal antiprism (D_{3d} symmetry) with angles that deviate from 90°, but with interatomic distances that remain equal in length. Quadratic distortion of the octahedron along a C_4 axis by compression or elongation creates a tetragonal dipyramid (D_{4h} symmetry) with angles that remain constant at 90°, but with interatomic distances that vary.

Mineral species with an MXY chemical formula, Z = 4, and a pyrite-type crystal structure have four metal atoms (4M) that occupy similar atomic positions in all three subgroups. These subgroups are differentiated according to the disorder or different ordering schemes of the eight nonmetal atoms (4X + 4Y) per unit cell that occupy similar atomic positions in all three subgroups (Bayliss, 1986).

The pyrite subgroup in the cubic space group $Pa3$ has 4M atoms that sit on the origin at the intersection of the threefold axes. The 4X and 4Y atoms are equally distributed (disordered) over the eight atomic positions on the threefold axes and may move along the threefold axes. The high symmetry and disorder are shown by the systematic absences of the 010 and 011 reflections in X-ray powder-diffraction patterns.

The ullmannite subgroup in the cubic space group $P2_13$ has 4M atoms on threefold axes near the origin. The 4X atoms are ordered in one set of four atomic positions on the threefold axes, and the 4Y atoms are ordered in the other set of four atomic positions on the threefold axes. The reduction in symmetry from cubic space group $Pa3$ to cubic space group $P2_13$ caused by nonmetal ordering allows each set of 4M or 4X or 4Y atoms to move along the threefold axes. Each M in a trigonal antiprism coordination moves along the threefold axis away from the larger 3X atoms and toward the smaller 3Y atoms. The lower symmetry of cubic space group $P2_13$ is shown by the systematic absence of the 010 reflection and the presence of the 011 reflection in X-ray powder-diffraction patterns.

The cobaltite subgroup is pseudocubic in the orthorhombic space group $Pca2_1$. The 4M, 4X, and 4Y atoms

0003–004X/89/0910–1168$02.00

Table 1. Octahedral bond angles and distances

Atoms	Ullmannite	Cobaltite
Y–M–Y	95°	87–96°
Y–M–X	85°	85–95°
X–M–X	95°	83–93°
M–X	2.38 Å	2.30 Å
M–Y	2.55 Å	2.36 Å

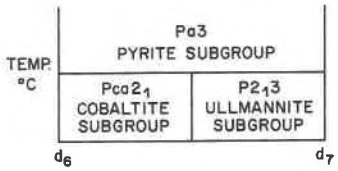

Fig. 1. Electronic and temperature stability of the pyrite subgroups.

are each ordered in a set of four atomic positions. The reduction in symmetry from $Pa3$ to $Pca2_1$ caused by nonmetal ordering allows each set of 4M or 4X or 4Y atoms to move off the threefold axes. Each M atom, which moves off the threefold axes, moves away from the larger 3X atoms and toward the smaller 3Y atoms. Each M atom retains trigonal antiprism coordination, because the angles deviate from 90° but the interatomic distances remain approximately equal in length (Table 1). The lower symmetry of the orthorhombic space group $Pca2_1$ is shown by the presence of the 010 and 011 reflections in X-ray powder-diffraction patterns.

The quadratic elongation of the octahedral site, determined by King and Prewitt (1979), is given in Table 2 and shows a maximum at FeS_2. A simple electronic theory for pyrite-type structures is proposed, where mineral species within the cobaltite subgroup are semiconductors (Hulliger, 1963) with a d^6 electronic configuration around the metal nucleus, whereas mineral species within the ullmannite subgroup are metallic with a d^7 electronic configuration around the metal nucleus. Both cobaltite ($Pca2_1$) heated at 850 °C and gersdorffite ($P2_13$) heated at 600 °C by Bayliss (1969) disordered into space group $Pa3$. The stability of the different subgroups, which are indicated in Figure 1, depends on the temperature and electronic structure. Therefore, the phases with the superstructures of Hulliger (1963) should be subdivided into cobaltite structure type if isoelectronic with cobaltite or ullmannite structure type if isoelectronic with ullmannite.

Tolovkite

Tolovkite (IrSbS), which was originally described by Razin et al. (1981), was assigned to the ullmannite subgroup on the basis of its X-ray powder-diffraction pattern and its isotropism. Because the strong 110 reflection of ullmannite is absent in tolovkite, intensities were calculated for tolovkite in each of the ullmannite-, pyrite-, and cobaltite-subgroup models in order to compare with the observed X-ray powder-diffraction intensities.

Razin et al. (1981) gave $a = 6.027(3)$ Å for tolovkite (PDF 35-656). A least-squares analysis of all 24 reflections except 410 and 511 gave $a = 6.025(2)$ Å with $F_{22} = 5.9(0.125,30)$ calculated by the method of Smith and Snyder (1979). The differences between $2\theta_{obs}$ and $2\theta_{calc}$ ($\Delta 2\theta$) are listed in Table 3. Since both the observed and calculated intensities show a strong 511 reflection, the 1.21° $\Delta 2\theta$ is attributed to a typographical error. Similarly, the 0.66° $\Delta 2\theta$ of the 410 reflection is attributed to a typographical error.

The atomic coordinates of tolovkite (Table 4) based upon the ullmannite ($P2_13$) subgroup model were derived from the 2.511-Å Sb-S interatomic distance and atomic positions of ullmannite by Pratt and Bayliss (1980). The atomic coordinates of tolovkite (Table 4) based upon the model for the pyrite ($Pa3$) subgroup were derived from the Sb and S atomic positions of the ullmannite-subgroup model set equidistance from the $x = 0.5$ position and the Ir set by symmetry at the origin.

The atomic coordinates of cobaltite by Bayliss (1982a) show that the (x, y, z) coordinates of Co move [−0.005, 0.010, 0.002] from the ideal position (0.0, 0.25, 0.0), whereas the atomic coordinates of both As and S in cobaltite show only minor movement from the ideal positions. The observed movement of Co from the ideal position agrees with the vector [−0.0055, 0.0092, 0.0018] predicted by the movement of Co away from the three small S atoms and toward the three larger As atoms on the basis of the observed interatomic distances within cobaltite.

The atomic coordinates of tolovkite (Table 4) based upon the model for the cobaltite ($Pca2_1$) subgroup were derived from the 2.511-Å Sb-S interatomic distance of ullmannite by Pratt and Bayliss (1980) with the Sb and S atomic positions set equidistance from the $x = 0.5$ position and ordered according to $Pca2_1$ symmetry. The Ir at the origin was moved away from the three small S atoms and toward the three larger Sb atoms on the basis of the observed Sb–S interatomic distances within ullmannite. The vector to convert coordinates of $Pa3$ to $Pca2_1$ is [0, 0.25, 0]. Values of the temperature factor B were selected to be similar to those of ullmannite.

The visually estimated observed intensities need to be systematically reduced as 2θ increases, because tolovkite has a large absorption coefficient. A comparison of the observed intensities with those of the model for the pyrite ($Pa3$) subgroup in Table 3 shows that the observed 310 reflection is not permitted in space group $Pa3$ and the observed reflections 221, 411, and 431 have calculated intensities of 0.00. A comparison of the observed intensities with those of the model for the ullmannite ($P2_13$) subgroup in Table 3 shows reflections not observed have

Table 2. Quadratic elongation of the octahedral site

MnS_2	FeS_2	CoS_2	NiS_2	CuS_2
1.0030	1.0061	1.0052	1.0039	1.0034

Table 3. X-ray powder-diffraction data of tolovkite

$h^2 + k^2 + l^2$	hkl	I_{calc} Pa3	I_{calc} $P2_13$	I_{calc} $Pca2_1$	I_{obs}	$\Delta 2\theta$
1	010	—	—	2.1*		
2	110	—	5*	0.9*		
3	111	6	6	7	6	0.08
4	200	7	10	8	9	−0.23
5	210	4	4	4	6	−0.06
6	211	3	4	4	6	0.16
8	220	5	6	5	8	−0.09
9	221, 300	0.00*	0.2	0.6	3	−0.25
10	310	—*	1.7*	0.2	1	0.10
11	311	10	10	10	10	−0.11
12	222	1.8	2.2	1.7	2	−0.24
13	320	0.8	1.5	1.1	3	−0.26
14	321	1.4	2.7	1.9	3	0.10
16	400	0.1	0.1	0.1		
17	410, 322	0.00	0.4	0.3	1	−0.66*
18	411, 330	0.00*	0.2	0.1	1	−0.01
19	331	1.5	1.8	1.5	4	−0.13
20	420	1.5	1.7	2.5	6	0.10
21	421	0.8	1.9*	0.9	2	0.20
22	332	0.4	0.4	0.4	3	−0.11
24	422	2.3	2.0	2.2	7	0.23
25	430, 500	0.00	0.3	0.03		
26	510, 431	0.00*	0.7	0.2	2	0.03
27	511, 333	5	5	5	9	−1.21*
29	520, 432	1.1	2.5	1.4	6	−0.09
30	521	0.7	1.3*	1.1		
32	440	4	4	4	9	−0.02
33	522, 441	0.0	1.4*	0.4		
34	530, 433	0.0	1.4*	0.3		
35	531	2.1	2.6	4	6	0.07
36	600, 442	6	5	6	8	0.10

* Unusual values discussed in text.

calculated intensities of 5 for 110, 1.3 for 521, 1.4 for 522, and 1.4 for 530. In addition, calculated intensities for 310 and 421 are significantly stronger than the observed intensities. A comparison of the observed intensities with those of the model for the cobaltite ($Pca2_1$) subgroup in Table 3 shows reflections not observed have calculated intensities of 2.1 for 010 and 0.9 for 110, although weak reflections in a strong background at low 2θ angles may not be observed.

The X-ray powder-diffraction data indicate that tolovkite belongs to the cobaltite subgroup rather than the ullmannite subgroup. This suggestion agrees with the theory summarized in Figure 1, since tolovkite is isoelectronic with cobaltite. In order to verify this suggestion, new X-ray diffraction data need to be collected.

Pyrite

The existence of two types of pyrite (isotropic and anisotropic) has been recognized for some time (e.g., Smith, 1942). The isotropic pyrite has a cubic crystal structure with space group $Pa3$ (Finklea et al., 1976) and the anisotropic pyrite has been shown to be pseudocubic (Bayliss, 1977a). Although the R of 3.2% for anisotropic pyrite in space group $P1$ (Bayliss, 1977a) is low, the table of structure factors shows poor agreement between F_{obs} and F_{calc} for the 132 reflections forbidden by space group $Pa3$. Therefore, although the deviation from cubic symmetry

Table 4. Atomic coordinates and temperature factors for tolovkite crystal-structure models

Atom(s)	Pa3 x	$P2_13$ x	$Pca2_1$ x	$Pca2_1$ y	$Pca2_1$ z	B
Ir	0.0	−0.0178	−0.0067	0.2612	0.0022	0.2
Sb		0.3891	0.3776	0.6276	0.3776	0.4
Sb + S	0.3776					0.6
S		0.6143	0.6224	0.8724	0.6224	0.8

is correct, the crystal-structure model does not adequately describe the fine detail.

Pyrite is isoelectronic with cobaltite. Figure 1 is consistent with the observations that the high-temperature phase (e.g., from a kyanite mine near York, South Carolina, U.S.A.) is isotropic with cubic space group $Pa3$ and also that the low-temperature phase (e.g., from Itaya mine, Yamagata Prefecture, Japan) is anisotropic with space group $Pca2_1$. A possible crystal-structure model to explain these observations is a sextuplet of interpenetrating, twin-related, orthorhombic (space group $Pca2_1$) domains about a $\bar{3}$ twin axis [111] as in cobaltite (Bayliss, 1982a), gersdorffite (Bayliss, 1982b), and ullmannite (Bayliss, 1986).

The relationship ΣF_{hk0} (k odd) = ΣF_{0kl} (l odd) = ΣF_{h0l} (h odd) indicates that the percentage of each pair of twins is similar. In Table 4 of Bayliss (1977a), the temperature factors of the atoms S(2), S(4), S(5), and S(7) are higher than those of the atoms S(1), S(3), S(6), and S(8). This ordering scheme matches III-$Pca2_1$ of Bayliss (1986), which indicates that one twin is more prominent than the other twin of this twin pair, III-$Pca2_1$.

The two sets of four S atoms in Table 4 of Bayliss (1977a) have atomic coordinates similar to those required by III-$Pca2_1$; however, the atomic coordinates of the Fe atoms show significant differences from those required by III-$Pca2_1$. In addition, the standard deviations of the atomic coordinates for S are less than those of Fe, whereas normally Fe should have smaller standard deviations than S, because Fe is heavier. These data on the Fe atoms indicate that minor adjustments should be made to the atomic coordinates of Fe.

The atomic coordinates (Table 5) of the model for the pyrite ($Pa3$) subgroup have been converted to identical positions in the model for the cobaltite ($Pca2_1$) subgroup. This cobaltite-subgroup model gives zero intensity for both 010 and 110 reflections. Minor variation of the unit-cell parameters a, b, and c had no effect on the intensities of the 010 and 110 reflections. Similarly, minor variation of the z parameter of the Fe, S(1), and S(2) atoms had no effect on the intensities of the 010 and 110 reflections. The x parameter of the Fe atom was most sensitive to the 110 reflection, whereas the y parameter of the Fe atom was most sensitive to the 010 reflection.

The vector predicted by the movement of the Fe atom away from the three S atoms with single bonds to Fe and toward the three S atoms with double bonds to Fe with

TABLE 5. Atomic coordinates for pyrite crystal-structure models

Atom	*Pa*3	*Pca*2$_1$			*Pca*2$_1$		
	x	*x*	*y*	*z*	*x*	*y*	*z*
Fe	0.0	0.0	0.25	0.0	−0.0049	0.2581	0.0016
S(1)	0.385	0.385	0.635	0.385	0.385	0.635	0.385
S(2)		0.615	0.865	0.615	0.615	0.865	0.615

the Fe–S interatomic distances of Pauling (1978) is [−0.0049, 0.0081, 0.0016], which produces the atomic coordinates given in Table 5. This crystal-structure model of a sextuplet of interpenetrating, twin-related, orthorhombic (space group *Pca*2$_1$) domains about a $\bar{3}$ twin axis [111] produces calculated intensities of reflections forbidden by space group *Pa*3 similar to the intensities observed by Bayliss (1977a).

An attempt to refine the data set from Bayliss (1977a) on the basis of this crystal-structure model was unsuccessful, because the atomic positions of each of the 12 sets of six atoms overlap signficantly. In addition, a few reflections are adversely affected by multiple diffraction. In order to verify this crystal-structure model, a data set needs to be refined from an untwinned crystal.

MASLOVITE

Maslovite (PtBiTe), which was originally described by Kovalenker et al. (1979), was assigned to the ullmannite subgroup on the basis of its X-ray powder-diffraction pattern and its isotropism. Because the strong 110 reflection of ullmannite is absent in maslovite, intensities were calculated for maslovite in each of the ullmannite- and pyrite-subgroup models in order to compare with the observed X-ray powder-diffraction intensities. The atomic coordinates of maslovite based upon the pyrite-subgroup (*Pa*3) model were derived as $Pt_{0.73}Pd_{0.27}$ (x = 0.0) and $Bi_{1.30}Te_{0.63}Sb_{0.07}$ (x = 0.369), whereas the atomic coordinates of maslovite based upon the ullmannite-subgroup (*P*2$_1$3) model were derived as $Pt_{0.73}Pd_{0.27}$ (x = −0.0048), Bi (x = 0.3684), and $Te_{0.63}Bi_{0.30}Sb_{0.07}$ (x = 0.627).

Kovalenker et al. (1979) gave a = 6.689(7) Å for maslovite; however, a least-squares analysis of all 15 reflections except 111 gave a = 6.687(3) Å with F_{14} = 4.5(0.129,24). The differences between $2\theta_{obs}$ and $2\theta_{calc}$ ($\Delta 2\theta$) are listed in Table 6. Since the observed intensity of the 111 reflection agrees with the calculated intensity, the 1.38° $\Delta 2\theta$ is attributed to a typographical error.

The calculated intensities in Table 6 are similar. Since the 110 reflection is not observed in maslovite as is required in *Pa*3 crystal-structure model, maslovite probably belongs to the pyrite subgroup. A disordered crystal structure is also suggested by significantly greater Bi than Te in the observed formula, $Pt_{0.73}Pd_{0.27}Bi_{1.30}Te_{0.63}Sb_{0.07}$, like gersdorffite-*Pa*3 where As is significantly greater than S (Bayliss, 1982b).

PENROSEITE AND VAESITE

Penroseite, $NiSe_2$, was originally described from Bolivia by Gorden (1926). The unit-cell dimensions of specimen ROM 19163 from the Hiaco mine, Colquechaca, Bolivia, and the Geological Survey of Canada (GSC) specimen from Paca Jake, Colquechaca, Bolivia, were measured by a Debye-Scherrer X-ray powder-diffraction camera. Unit-cell dimensions were calculated with the function of Nelson and Riley (1945) for ROM 19163 as 6.0132 Å and for GSC as 6.0154 Å. The data (PDF 6-507) of Earley (1950) yield a unit-cell dimension of 5.9923(11) Å by least-squares with F_{27} = 10.7(0.059,43), whereas Furuseth and Kjekshus (1969) gave 5.9629 Å for pure $NiSe_2$.

Vaesite, NiS_2, was originally described from the Kasompi mine, Shinkolobwe, Katanga, Zaire, by Kerr (1945). The Geological Survey of Canada specimen from the type locality has a unit-cell dimension of 5.670 Å, identical to that of the type specimen (PDF 11-99), but smaller than 5.6873 Å for pure NiS_2 (Furuseth and Kjekshus, 1969). Because the specimen also contained both linnaeite and pyrite, the chemical composition of vaesite was determined by electron microprobe (Table 7).

From each of these three specimens, small crystal fragments about 20 μm in size were selected to reduce the possibility of chemical zoning. Precession photographs were taken of these small crystal fragments to find single

TABLE 6. X-ray powder-diffraction data of maslovite

$h^2 + k^2 + l^2$	*hkl*	I_{calc} *Pa*3	I_{calc} *P*2$_1$3	I_{obs}	$\Delta 2\theta$
2	110	—	4*		
3	111	7	7	1	−1.38*
4	200	20	23	1	−0.14
5	210	100	100	10	0.25
6	211	72	74	8	−0.32
8	220	23	23	2	−0.09
9	221	1	1		
10	310	—	1		
11	311	86	87	6	0.12
12	222	8	9	1	−0.08
13	230	18	21	2	−0.10
14	321	42	43	3	0.04
16	400	4	5		
17	410, 322	1	1		
18	411, 330	0	0		
19	331	0	0		
20	420	14	13	1	−0.08
21	421	22	23	1	−0.01
22	332	9	10		
24	422	7	8		
25	430	0	0		
26	510, 431	0	1		
27	511, 333	23	24	2	−0.09
29	250, 432	18	19	1	0.38
30	521	11	11	1	−0.10
32	440	22	22	2	−0.01

* Unusual value discussed in text.

Table 7. Electron-microprobe analyses of bravoite, vaesite, cattierite, and fukuchilite

Specimen and locality	Fe	Ni	Co	Cu	As	S	Total
Bravoite: BM 1940,82	32.9	12.9	0.9		0.2	52.6	99.5
Mill Close mine, England	31.1	14.4	1.0		0.3	52.8	99.6
Bravoite: BM 1925,886	42.2	1.7	0.3		0.6	52.3	97.1
Mechernich, East Germany	35.3	9.7	0.1		0.5	53.1	98.7
Bravoite: BM 1940,43	36.9	8.6	0.1		0.2	53.1	98.9
Mill Close mine, England	28.9	16.5	0.3		0.2	53.1	99.0
Vaesite: GSC	0.9	43.9	1.6		0.0	51.8	98.2
Shinkolobwe, Zaire	0.9	44.8	1.4		0.1	51.6	98.8
Cattierite: BM 1971,92	4.7	4.9	38.0			52.3	99.9
Shinkolobwe, Zaire	6.5	2.9	38.0			52.2	99.6
Fukuchilite	15.7			33.4		50.9	100.0
Hanawa mine, Japan	15.4			33.5		51.2	100.1
	15.2			33.6		50.3	99.1
	14.8			34.0		51.4	100.2
	15.1			34.2		50.9	100.2
	13.8			35.5		50.9	100.2
	12.9			36.4		50.7	100.0
	12.7			37.0		50.1	99.8

crystals. Intensities and unit-cell dimensions from each of these three specimens were measured on a four-circle diffractometer. The absence of 24 reflections forbidden by space group $Pa3$ confirmed the systematic absences of the pyrite subgroup for all specimens.

Bravoite

A highly nickeliferous (Ni 18 wt%) pyrite, $(Fe_{0.62}Ni_{0.38})S_2$, from Minasragra, near Cerro de Pasco, departamento Junin, Peru, was originally described by Hillebrand (1907), who stated, "Should it seem proper to give it a specific name later, bravoite is suggested." X-ray powder-diffraction data (PDF 2-850) from the type locality are given by Harcourt (1942). A unit-cell dimension of 5.569(1)KX was derived by least-squares with $F_{20} = 7.8(0.086,30)$ of Smith and Snyder (1979), and the systematic absences agree with space group $Pa3$. Further descriptions of bravoite from Minasragra have been made by Clark and Kullerud (1963) and Moh and Ottemann (1964).

The chemical compositions of minerals within FeS_2-CoS_2-NiS_2 from the literature are plotted on a triangular diagram by Klemm (1965). Strong chemical zoning within individual specimens has been demonstrated by Moh and Ottemann (1964), Ixer (1978), Watkinson et al. (1975), and Vaughan (1969). Klemm (1965) gave 25 electron-microprobe analyses between FeS_2 and $(Fe_{0.35}Ni_{0.65})S_2$ from Mechernich specimens and 12 electron-microprobe analyses between $(Fe_{0.87}Ni_{0.13})S_2$ and $(Fe_{0.35}Ni_{0.65})S_2$ from Divrik, Turkey, specimens. Therefore, natural specimens indicate complete solid solution within the FeS_2-CoS_2-NiS_2 system. Unit-cell dimensions (Clark and Kullerud, 1963) intermediate between pyrite and vaesite confirm the solid solution.

The compositional gap, $(Fe_{0.8}Ni_{0.2})S_2$-$(Fe_{0.5}Ni_{0.5})S_2$, determined synthetically at 700 °C in a LiCl-KCl flux by Klemm (1965), is significantly smaller than that of $(Fe_{0.93}Ni_{0.07})S_2$-$(Fe_{0.24}Ni_{0.76})S_2$ in a fluxless synthesis by Clark and Kullerud (1963), which illustrates the difficulty of attaining equilibrium. Complete solid solution was obtained at 200 °C in acidic solutions by Springer et al. (1964), whereas Clark and Barnes (1965) discussed synthetic $(Fe_{0.5}Ni_{0.5})S_2$ formed under 137 °C in an alkali solution. Because of the difficulty of attaining equilibrium, Shimazaki (1971) interpreted the above-mentioned experimental results to mean that thermochemically stable $(Fe_{0.5}Ni_{0.5})S_2$ with fixed composition below 137 °C does not exist.

Natural specimens of bravoite were obtained as follows: BM1940,28 (type locality); BM1925,886; BM1940,43; and BM1940,82 (Table 7). Bravoite from Mechernich, Euskirchen, Rhennish Prussia, has been described by Clark and Kullerud (1963), Moh and Ottemann (1964), and Klemm (1965). Bravoite from Mill Close mine, Darley Dale, Derbyshire, England, has been described by Bannister (1940), Clark and Kullerud (1963), and Vaughan (1969).

Electron-microprobe analyses of bravoite in Table 7 confirm the strong chemical zoning reported in the literature. Minor amounts of As are reported similar to that in the chemically zoned bravoite from Saskatchewan by Watkinson et al. (1975). Bravoite crystals were examined to check whether the type specimen is isostructural with pyrite and also to check whether other minerals with similar composition are also isostructural with pyrite. Many small crystal fragments of each specimen about 20 μm in size were selected to reduce the possibility of chemical zoning. Precession photographs were taken of these small crystal fragments to find single crystals. Intensities and unit-cell dimensions were measured on single crystals on a four-circle diffractometer. The absence of 24 reflections forbidden by space group $Pa3$ confirmed the systematic absences of the pyrite subgroup for all specimens.

The unit-cell dimension of 5.567 Å for a bravoite single crystal from Mechernich predicts a chemical composition

of $(Ni_{0.58}Fe_{0.42})S_2$ based upon a uniform unit-cell dimension change with composition from FeS_2 (5.4281 Å) to NiS_2 (5.6873 Å) established by Klemm (1962). This composition is identical to that determined by Springer et al. (1964). The unit cell of 5.537 Å for a bravoite single crystal from the Mill Close mine predicts a chemical composition of $(Fe_{0.54}Ni_{0.46})S_2$, which is more Ni-rich than given by Bannister (1940); however, the specimen is zoned. Therefore, there is a complete solid-solution series between pyrite and vaesite with the pyrite structure type.

On the basis of the general guideline implied by Nickel and Mandarino (1987) that there should only be one mineral name per end-member formula with a specific structure type, $(Fe,Ni)S_2$ with a pyrite structure type should be called nickeloan pyrite. Therefore, the name nickeloan pyrite should be used instead of bravoite (Fig. 2). This nomenclature has been accepted by the International Mineralogical Association Commission on New Minerals and Mineral Names (IMA-CNMMN).

Villamaninite

The crystal-structure determination of CuS_2 by King and Prewitt (1979) in space group *Pa*3 established a pyrite structure type. The unit-cell dimension of CuS_2 with a pyrite structure type has been determined by Krill et al. (1976), Bither et al. (1968), Taylor and Kullerud (1972), and King and Prewitt (1979) as a = 5.7900(4), 5.7898(5), 5.7897(2), and 5.7891(6) Å, respectively. A unit-cell dimension of a = 5.625 Å at 80-kbar pressure has been determined by Hinze and Will (1980). Krill et al. (1976) have established that CuS_2 is stoichiometric. The pressure-temperature diagram of Taylor and Kullerud (1972) indicates that CuS_2 is metastable at room temperature below 8-kbar pressure.

Villamaninite from Villamanin, Cármenes, León, Spain, was named and chemically analyzed by Schoeller and Powell (1920) as $Cu_{0.43}Ni_{0.33}Co_{0.13}Fe_{0.11}S_2$ and by Hey (1962) as $Cu_{0.51}Ni_{0.27}Fe_{0.13}Co_{0.09}S_2$. Within this deposit, Ypma (1968) showed that there are three cubic minerals: cuprian bravoite $Fe_{0.55}Ni_{0.22}Cu_{0.12}Co_{0.11}S_2$ with a = 5.59–5.62 Å, nodular villamaninite $Ni_{0.35}Cu_{0.28}Fe_{0.26}Co_{0.11}S_2$ with a = 5.65–5.67 Å, and idiomorphic villamaninite $Cu_{0.60}Fe_{0.23}Ni_{0.14}Co_{0.03}S_2$ with a = 5.69–5.705 Å. Then Ypma et al. (1968) proposed that the definition of villamaninite be a mineral species with a pyrite structure type that contains more than 25 and less than 75 mol% CuS_2.

Villamaninite from Villamanin studied by La Iglesia et al. (1974) gave a = 5.6911(1) Å for $(Cu_{0.49}Ni_{0.33}Co_{0.13}Fe_{0.06})S_2$. A uniform unit-cell change with composition has been established from FeS_2 to CuS_2 by Shimazaki and Clark (1970) and from FeS_2 to NiS_2 by Klemm (1962). The composition of $Cu_{0.7}Fe_{0.3}S_2$ on the CuS_2-FeS_2 versus unit-cell dimension curve of Shimazaki and Clark (1970) has a unit-cell dimension similar to villamaninite from Villamanin with formula $(Cu_{0.60}Fe_{0.23}Ni_{0.14}Co_{0.03})S_2$, and a = 5.6944(3) Å (Bayliss, 1977b) with F_{17} = 49.6(0.0163,21) of Smith and Snyder (1979). The Ni content of villamaninite will have negligible effect on the unit-cell dimension, because NiS_2 has a similar unit-cell dimension, a = 5.6873(5) Å (Furuseth and Kjekshus, 1969), to villamaninite. Therefore, the composition and unit cell of villamaninite is similar to that predicted by the CuS_2-FeS_2 versus unit-cell dimension curve of Shimazaki and Clark (1970).

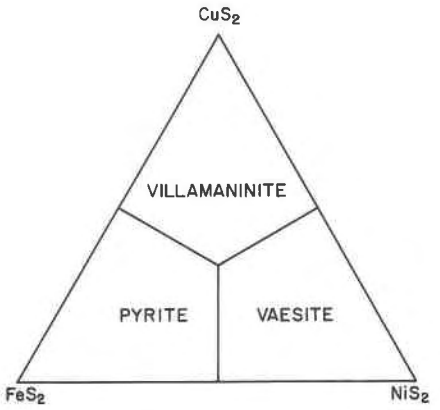

Fig. 2. Mineral names within the FeS_2-NiS_2-CuS_2 system.

Small crystal fragments, about 20 μm in size, of villamaninite from Villamanin, $(Cu,Ni,Co,Fe)S_2$, (ROM M12668) were selected to reduce the possibility of chemical zoning. Precession photographs were taken of these small crystal fragments to find a single crystal. Intensities and a unit-cell dimension were measured for this single crystal on a four-circle diffractometer. The unit-cell dimension of 5.678 Å confirms a chemical ratio of Cu:Fe = 2:1 based upon the CuS_2-FeS_2 versus unit-cell dimension curve of Shimazaki and Clark (1970). The absence of 24 reflections forbidden by space group *Pa*3 confirmed the systematic absences of the pyrite subgroup. The broad reflections of the powder-diffraction pattern as well as most crystal fragments indicate strong chemical zoning.

In 1986, a new mineral name was proposed for the CuS_2 end-member mineral. This proposal was opposed by J. A. Mandarino, because he felt that villamaninite was considered to include end-member CuS_2. Another occurrence of end-member CuS_2 has been identified in black-smoker specimens from the Juan de Fuca Ridge and has been called villamaninite by A. C. Roberts (personal communication), and an unnamed mineral from the Providencia mine, León, Spain described by Paniagua (1989) appears to be villamaninite as well.

On the basis of the general guideline implied by Nickel and Mandarino (1987) that there should only be one mineral name per end-member formula with a specific structure type, villamaninite is defined to have an end-member composition of CuS_2 with a pyrite structure type in space-group *Pa*3, as illustrated by Figure 2. This nomenclature has been accepted by the IMA-CNMMN.

Fukuchilite

Fukuchilite from the type locality of Hanawa mine, Akita Prefecture, Japan, was originally described by Ka-

TABLE 8. X-ray powder-diffraction data of fukuchilite, villamaninite, and ordered and disordered calculated models

		Fukuchilite							
		Kajiwara (1969)		Shimazaki (1971)		This work	Villa-maninite	Ordered	Disordered
$h^2 + k^2 + l^2$	*hkl*	$\Delta 2\theta$	I_{obs}	$\Delta 2\theta$	I_{obs}	I_{obs}	I_{obs}	I_{calc}	I_{calc}
1	100							0.5	
2	110	0.113*	vvw					0.5*	
3	111	−0.037	s	−0.221	wb	20	15	24	24
4	200	−0.001	vs	0.049	sb	100	100	100	100
5	210	0.034	w	−0.253	wb	10	30	34	37
6	211	0.061	m	−0.259	vwb	2	25	39	34
8	220	−0.042	w	−0.166	wb	5	25	49	49
9	300, 221							1	2
10	310							0.1	
11	311	0.088	s	−0.071	wb	10	40	79	79
12	222						5	15*	15
13	230	−0.090	w			5	10	16	16
14	321						10	21	20
16	400							0	0
17	140, 322						2	2	2
18	411, 330						1	2	1
19	331			−0.201	vwb		5	13	13
20	420						3	9	9
21	421						1	6	5
22	332							2	2
24	422						3	11	11
25	430, 500						1	1	2
25	431, 510							2	2
26	333, 511			0.323	vwb		15	35	35

* Unusual value discussed in text.

jiwara (1969) with pyrite and covellite. The chemical formula was derived from 24 electron-microprobe analyses with Cu 37.9–40.6, Fe 10.5–12.9, and S 49.2–53.3 wt% to give a formula close to Cu_3FeS_8 (Cu 37.9, Fe 11.1, S 51.0 wt%). Although Kajiwara (1969) stated that "the S/Cu + Fe atomic ratio lies in the range between 1.7 and 2.1," calculations with his electron-microprobe analyses give the ratio between 1.95 and 2.04. Pyrite-type minerals have only been described as stoichiometric phases and are expected to be stoichiometric (Krill et al., 1976). Experimental data of Bayliss (1982a, 1982b, 1986) gave a sulfur:metal experimental error variability of 1.98 to 2.02 for pyrite-type minerals. Kajiwara (1969) stated that "The Cu/Fe atomic ratio is nearly equal to 3.0," which is confirmed by calculations that give $(Cu_{0.72}Fe_{0.28})$ to $(Cu_{0.77}Fe_{0.23})$.

The chemical analyses of the mixtures in Table 2 of Kajiwara (1969) calculate out to be 69.6 FeS_2, 9.6 CuS_2, and 20.8 CuS mol%. His paper does not explain the discrepancy between these values and the different percentages used two pages later in "a pycnometer determination of a mixture containing about 50% pyrite, 35% fukuchilite, and 15% covellite in volume percentage."

Shimazaki and Clark (1970) gave Fe 28.9(1), Cu 23.4(2), and S 47.7(2) wt% for a fukuchilite, pyrite, and covellite mixture (≅40 μm) by electron microprobe, because an area of fukuchilite large enough (>1 μm) to be analyzed could not be found. This electron-microprobe analysis represents 62 FeS_2, 11 CuS_2, and 27 CuS mol%. Since the electron beam penetrates significantly greater than 1 μm, most of the grains chemically analyzed are below the surface, where the modal analyses were carried out. Since the fukuchilite-bearing masses are heterogeneous as shown by the microphotographs of Kajiwara (1969), the modal analyses are unsound. Shimazaki and Clark (1970) stated, "In the experiments, a pinkish colour was observed with the more copper-rich phases" and "the natural fukuchilite is pinkish grey in colour." The pinkish color suggests that fukuchilite has a higher Cu/Fe ratio rather than a lower S/(Cu + Fe) ratio.

Yui (1972) gave Fe 12.3, Cu 38.0, and S 50.1 wt% for fukuchilite, which represents Cu:Fe = 2.72 $(Cu_{0.73}Fe_{0.27})$. Yui (1972) stated, "uncertainty remains in [the] possible occurrence of an iron-rich mineral hidden under the polished surface at the anlayzed spot, and/or in a possibility of fukuchilite being a mixture of two or more phases in the Cu-Fe-S system." Another phase with Cu:Fe = 1.7 $(Cu_{0.63}Fe_{0.37})$ was found; however, the S/(Cu + Fe) ratios of both phases are about 2.

A fukuchilite specimen from the type locality supplied by Dr. Yui contains a grayish mineral up to 20 μm wide, which is fukuchilite on the basis of its optical description. The fukuchilite is shown by backscattered-electron photographs to be compositionally zoned. Eight electron-microprobe analyses are given in Table 7. Seven electron-microprobe analyses were taken in areas void of chemical zoning and unreacted pyrite, whereas the low S content of the last analysis indicates a fukuchilite-covellite mixture. The data shows minor Cu-Fe chemical zoning from $Cu_{0.67}Fe_{0.34}S_{1.99}$ to $Cu_{0.72}Fe_{0.29}S_{1.99}$. In addition, chalcopyrite was identified in the fukuchilite-bearing mass.

Conclusions from all chemical data are that fukuchilite

is stoichiometric with a $(Cu,Fe)S_2$ formula. The Cu-Fe chemical zoning is recorded from $Cu_{0.63}Fe_{0.37}$ to $Cu_{0.77}Fe_{0.23}$.

The unit-cell dimension of 5.58 Å from Kajiwara (1969) is similar to 5.60(1) Å from Shimazaki and Clark (1970), who stated that the reflections were weak and broad. A powder pattern was taken of a fukuchilite-bearing mass supplied by Dr. Kajiwara with similar proportions of pyrite, covellite, and fukuchilite to that used by Kajiwara (1969). A diffractometer with monochromatic Fe$K\alpha$ radiation at 40 kV and 20 mA was used with 50-s count times at 0.1° 2θ intervals. The broad asymmetrical reflections in the powder pattern of fukuchilite were confirmed and indicate chemical zoning with a unit-cell dimension range from 5.62 to 5.58 Å. Strong chemical zoning has been observed in many minerals with the pyrite structure type (Bayliss, 1986); therefore, chemical zoning is expected within the CuS_2-NiS_2-CoS_2-FeS_2 system. Minerals with a variety of compositions have been reported in this system by Zakrzewski (1984).

The wavelength used by Kajiwara (1969) to convert 2θ into d spacings was calculated to be 1.5398(9) Å; however, even with this unusual wavelength, one d spacing was too large, whereas two d spacings were too small. The 2θ angles of Kajiwara (1969) were not corrected with an internal or external standard, because the 2θ errors are random. The differences are attributed to a calculation error. A least-squares refinement of the 2θ angles of fukuchilite by Kajiwara (1969) with Cu$K\alpha$ radiation of 1.54184 Å gave a unit-cell dimension of 5.585(3) Å.

The X-ray powder-diffraction intensities of fukuchilite (Kajiwara, 1969; Shimazaki and Clark, 1970) are similar to those of villamaninite (Bayliss, 1977b) in Table 8. Therefore fukuchilite has a pyrite structure type. A lower symmetry than pyrite was suggested because of a very very weak peak at 22.4° 2θ; however, this suggested 110 reflection has the largest 2θ error at 1.8σ. The F_7 = 15.5(0.050,9) of Smith and Snyder (1979) for the model of the pyrite structure type, $(Cu,Fe)S_2$, drops to F_8 = 12.5(0.058,11) for the low-symmetry crystal-structure model Cu_3FeS_8 of Kajiwara (1969). The maximum effect on the X-ray powder-diffraction data would be caused by complete ordering of Cu in space group $P1$, although Cu ordering with trigonal symmetry is also possible. Table 8 shows calculated patterns for both the metal-atom-ordered ($P1$) and metal-atom-disordered models ($Pa3$) with (Cu,Fe) at x = 0.0 and S at x = 0.3951. Since the 222 reflection at 57.13° 2θ is not observed in fukuchilite, the 110 reflection calculated at less than one-tenth of the intensity of 222 should also not be observed.

The 110 reflection was not observed in powder-diffraction patterns by Shimazaki and Clark (1970) or in the present study (Table 8). A number of low-quality fukuchilite crystal fragments, which were examined with a precession camera, did not show a 110 reflection. Since the specimen used by Kajiwara (1969) contained 70 mol% FeS_2 as well as fukuchilite, a high background occurs owing to fluorescence of Fe in the specimen by Cu radiation. Therefore the very very weak peak on the diffractometer chart at 22.4° 2θ is probably less than 1σ above background and represents the normal random statistical production of X-rays.

With ideal-solution behavior between FeS_2 (pyrite) and CuS_2 (synthetic), the unit-cell dimension of $Cu_{0.75}Fe_{0.25}S_2$ would be 5.70 Å, whereas the unit-cell dimension of fukuchilite is 5.60(2) Å. Such large deviations from ideal behavior are unusual, and ordering phenomena is a possible explanation. At present, there is no evidence for metal ordering within pyrite-type minerals in the CuS_2-NiS_2-CoS_2-FeS_2 system.

No anisotropism was observed under crossed Nicols by Kajiwara (1969). An optically isotropic cubic mineral like fukuchilite cannot have an ordered-metal-atom pyrite-type crystal structure, which requires a triclinic or trigonal crystal system.

Because fukuchilite heated for 2 d at 200 °C remained unchanged, Kajiwara (1969) suggested that Cu_3FeS_8 is stable below 200 °C. This experiment does not represent equilibrium, however, because 112 d was used by Shimazaki and Clark (1970), who noted the sluggish exsolution of Cu from the pyrite structure type. In addition, no exact composition was found in their low-temperature hydrothermal synthesis as solid solution was found from FeS_2 to $(Fe_{0.18}Cu_{0.82})S_2$ including zoned crystals. The existence of a continuous solid solution $(Cu,Fe)S_2$ and the absence of a thermodynamically stable Cu_3FeS_8 phase indicates that a separate Cu_3FeS_8 phase does not exist.

Fukuchilite is $(Cu,Fe)S_2$ with a pyrite structure type (space group $Pa3$) and a variable Cu/Fe ratio. Fukuchilite is different from villamaninite from Villamanin, which contains minor Ni and Co. Therefore, the reflected-light optics (Criddle and Stanley, 1986) and the unit-cell dimension (Bayliss, 1977b) of villamaninite are slightly different from those of fukuchilite.

Villamaninite has recently been accepted by the IMA-CNMMN as a mineral with a pyrite structure type and the end-member formula of CuS_2 in the system CuS_2-NiS_2-CoS_2-FeS_2 on the basis of historical precedent. A proposal to discredit fukuchilite as equivalent to villamaninite was rejected by IMA-CNMMN, because there is not sufficient evidence as yet to discredit a mineral that was accepted by the IMA-CNMMN.

Acknowledgments

Financial assistance was provided by the National Sciences and Engineering Research Council of Canada. Mr. R. Rutherford did some of the electron-microprobe analyses, whereas Dr. D. C. Harris did the electron-microprobe analyses of fukuchilite. Dr. E. H. Nickel, vice chairman of the IMA-CNMMN, provided valuable advice. Dr. E. Petersen provided a critical review.

References cited

Bannister, F.A. (1940) Bravoite from Mill Close mine, Derbyshire, Mineralogical Magazine, 25, 609–614.

Bayliss, P. (1969) X-ray data, optical anisotropism, and thermal stability of cobaltite, gersdorffite, and ullmannite. Mineralogical Magazine, 37, 26–33.

——— (1977a) Crystal structure refinement of a weakly anisotropic pyrite. American Mineralogist, 62, 1168–1172.

——— (1977b) X-ray powder data for villamaninite. Mineralogical Magazine, 41, 545.

——— (1982a) A further crystal structure refinement of cobaltite. American Mineralogist, 67, 1048–1057.

——— (1982b) A further crystal structure refinement of gersdorffite. American Mineralogist, 67, 1058–1064.

——— (1986) Subdivision of the pyrite group, and a chemical and X-ray diffraction investigation of ullmannite. Canadian Mineralogist, 24, 27–33.

Bither, T.A., Bouchard, R.J., Cloud, W.H., Donohue, P.C., and Siemons, W.J. (1968) Transition metal pyrite dichalcogenides. High-pressure synthesis and correlation of properties. Inorganic Chemistry, 7, 2208–2220.

Clark, L.A., and Barnes, H.L. (1965) Metastable solid solution relations in the system FeS_2-CoS_2-NiS_2 (discussion). Economic Geology, 60, 181–182.

Clark, L.A., and Kullerud, G. (1963) The sulfur-rich portion of the Fe-Ni-S system. Economic Geology, 58, 853–885.

Criddle, A.J., and Stanley, C.J. (1986) The quanitative data file for ore minerals. British Museum (Natural History), London.

Earley, J.W. (1950) Description and synthesis of the selenide minerals. American Mineralogist, 35, 337–364.

Finklea, S.L., III, Cathey, L., and Amma, E.L. (1976) Investigation of the bonding mechanism in pyrite using the Mössbauer effect and X-ray crystallography. Acta Crystallography, A32, 529–537.

Furuseth, S., and Kjekshus, A. (1969) On the magnetic properties of $CoSe_2$, NiS_2, and $NiSe_2$. Acta Chemica Scandinavica, 23, 2325–2334.

Gorden, S.G. (1926) Penroseite and trudellite: Two new minerals. Proceedings of the Academy of Natural Science of Philadelphia, 77, 317–324.

Harcourt, G.A. (1942) Tables for the identification of ore minerals by X-ray powder patterns. American Mineralogist 27, 63–113.

Hey, M.H. (1962) A new analysis of villamaninite. Mineralogical Magazine, 33, 169–170.

Hillebrand, W.F. (1907) The vanadium sulphide, patronite, and its mineral associates from Minasragra, Peru. American Journal Science, fourth series, 24, 141–151.

Hinze, E., and Will, G. (1980) Diffusion and decomposition in the pressure gradient of a diamond anvil squeezer. Neues Jahrbuch für Mineralogie Monatshefte, 481–497.

Hulliger, F. (1963) New compounds with cobaltite structure. Nature, 198, 382–383.

Ixer, R.A. (1978) The distribution of bravoite and nickeliferrous marcasite in central Britain. Mineralogical Magazine, 42, 149–150.

Kajiwara, Y. (1969) Fukuchilite, Cu_3FeS_8, a new mineral from the Hanawa mine, Akita prefecture, Japan. Mineralogical Journal (Japan), 5, 399–416.

Kerr, P.F. (1945) Cattierite and vaesite: New Co-Ni minerals from the Belgian Congo. American Mineralogist, 30, 483–497.

King, H.E., Jr., and Prewitt, C.T. (1979) Structure and symmetry of CuS_2 (pyrite structure). American Mineralogist, 64, 1265–1271.

Klemm, D. (1962) Untersuchungen über die Mischkristallbildung im Dreieckdiagramm FeS_2-CoS_2-NiS_2 und ihre Beziehungen zum Aufbau der natürlichen "Bravoite." Neues Jahrbuch für Mineralogie Monatschefte, 76–91.

——— (1965) Synthesen und Analysen in den Dreiecksdiagrammen FeAsS-CoAsS-NiAsS und FeS_2-CoS_2-NiS_2. Neues Jahrbuch für Mineralogie Abhandlungen, 103, 205–255.

Kovalenker, V.A., Berizov, V.D., Evstigneeva, T.L., Troneva, N.V., and Ryabikin, V.A. (1979) Maslovite, PtBiTe: A new mineral from the October copper-nickel deposit. Geologiya Rudnix Mestorozhdenii, 21, 94–104 (in Russian).

Krill, G., Panissod, P., Lapierre, M.F., Gautier, F., Robert, C., and Nassr Eddine, M. (1976) Magnetic properties and phase transistions of the metallic CuX_2 dichalcogenides (X = S, Se, Te) with pyrite structure. Journal of Physics C: Solid State Physics, 9, 1521–1533.

La Iglesia, A., Caballero, M.A., and Menendez del Valle, F. (1974) Estudio mineralogico de la villamaninita (Cu,Ni,Co,Fe) $(Se,S)_2$. Boletin Geológico y Mineralogico, 85, 436–441.

Moh, G.H., and Ottemann, J. (1964) X-ray fluorescence and electron-probe analyses of pyrite-type minerals. Carnegie Institution of Washington Year Book 63, 214–216.

Nelson, J.B., and Riley, D.P. (1945) An experimental investigation of extrapolation methods in the derivation of accurate unit-cell dimensions of crystals. Proceedings of the Physical Society, 57, 160–177.

Nickel, E.H., and Mandarino, J.A. (1987) Procedures involving the IMA Commission on New Minerals and Mineral Names and guidelines on mineral nomenclature. American Mineralogist, 72, 1031–1042; Errata (1988) 73, 200.

Paniagua, A. (1989) The pyrite-type Cu-rich disulfides in the Providencia mine, Leon, NW Spain. Neues Jahrbuch für Mineralogie Abhandlungen, 160, 8–11.

Pauling, L. (1978) Covalent chemical bonding of transition metals in pyrite, cobaltite, skutterudite, millerite and related minerals. Canadian Mineralogist, 16, 447–452.

Pratt, J.L., and Bayliss, P. (1980) Crystal structure refinement of a cobaltian ullmannite. American Mineralogist, 65, 154–156.

Razin, L.V., Rudashevsky, N.S., and Sidorenko, G.A. (1981) Tolovkite, IrSbS, a new sulfoantimonide of iridium from northeastern USSR. Zapiski Vsesoyuznoye Mineralogy Obshchestvo, 110, 474–480 (in Russian).

Robinson, K., Gibbs, G.V., and Ribbe, P.H. (1971) Quadratic elongation: A quantitative measure of distortion in coordination polyhedra. Science, 172, 567–570.

Schoeller, W.R., and Powell, A.R. (1920) Villamaninite, a new mineral. Mineralogical Magazine, 19, 14–18.

Shimazaki, H. (1971) Thermochemical stability of bravoite. Economic Geology, 66, 1080–1082.

Shimazaki, H., and Clark, L.A. (1970) Synthetic FeS_2-CuS_2 solid solution and fukuchilite-like minerals. Canadian Mineralogist, 10, 648–664.

Smith, F.G. (1942) Variation in the properties of pyrite. American Mineralogist, 27, 1–17.

Smith, G.S., and Snyder, R.L. (1979) F_N: A criterion for rating powder diffraction patterns and evaluating the reliability of powder-pattern indexing. Journal of Applied Crystallography, 12, 60–65.

Springer, G., Schachner-Korn, D., and Long, J.V.P. (1964) Metastable solid solution relations in the system FeS_2-CoS_2-NiS_2. Economic Geology, 59, 475–491.

Taylor, L.A., and Kullerud, G. (1972) Phase equilibria associated with the stability of copper disulfide. Neues Jahrbuch für Mineralogie Monatshefte, 458–464.

Vaughan, D.J. (1969) Zonal variation in bravoite. American Mineralogist, 54, 1075–1083.

Watkinson, D.H., Heslop, J.B., and Ewert, W.D. (1975) Nickel sulphide-arsenide assemblages associated with uranium mineralization, Zimmer Lake area, northern Saskatchewan. Canadian Mineralogist, 13, 198–204.

Ypma, P.J.M. (1968) Pyrite group: An unusual member: $Cu_{0.60}Ni_{0.14}Co_{0.03}$-$Fe_{0.23}S_2$. Science, 159, 194.

Ypma, P.J.M., Evers, H.J., and Woensdregt, C.F. (1968) Mineralogy and geology of the Providencia mine (León, Spain), type-locality of villamaninite. Neues Jahrbuch für Mineralogie Monatshefte, 174–191.

Yui, S. (1972) Quantitative electron-probe microanalysis of sulphide minerals. In G. Shinoda, K. Kohra, and T. Ichinokawa, Eds. Proceedings, Sixth International Conference on X-ray Optics and Microanalysis, p. 749–753. University of Tokyo Press, Tokyo.

Zakrzewski, M.A. (1984) Minerals of the bravoite-villamaninite series and cuprian siegenite from Karniowice, Poland. Canadian Mineralogist, 22, 499–502.

Manuscript received November 17, 1988
Manuscript accepted May 17, 1989